

# Antibodies@MOFs: An In Vitro Protective Coating for Preparation and Storage of Biopharmaceuticals

Yifan Feng, Huanrong Wang, Sainan Zhang, Yu Zhao, Jia Gao, Yunyi Zheng, Peng Zhao, Zhenjie Zhang, Michael J. Zaworotko, Peng Cheng, Shengqian Ma,\* and Yao Chen\*

Antibodies have emerged as a fast-growing category of biopharmaceuticals that have been widely applied in scientific research, medical diagnosis, and disease treatment. However, many antibodies and other biopharmaceuticals display inferior biophysical properties, such as low stability and a propensity to undergo aggregation. Enhancing the stability of biopharmaceuticals is essential for their wide applications. Here, a facile in vitro protective coating strategy based on metal–organic frameworks (MOFs) is proposed to efficiently protect antibodies against perturbation environments and quickly recover them from the MOFs before usage, which avoids introducing protective additives into the body, which may cause biosafety risks. The protected antibodies exhibit extraordinary thermal, chemical, and mechanical stabilities, and they can survive for long-term storage (>3 weeks) under severe temperature variation (4 ↔ 50 °C) at a fast ramp rate (25 °C min<sup>-1</sup>). More importantly, the encapsulated antibodies can be easily released as quickly as 10 s with high efficiency (≈100%) to completely remove the MOFs before use. This study paves a new avenue for the facile preparation and storage of biopharmaceuticals represented by antibodies under ambient or perturbation conditions, which may greatly broaden and promote the applications of both MOFs and biopharmaceuticals.

Biopharmaceuticals<sup>[1]</sup> have emerged as significant tools in the treatment of a broad spectrum of diseases.<sup>[2]</sup> For instance, antibodies are essential immunoglobulin molecules that become a fast-growing category of therapeutic proteins,<sup>[3]</sup> and widely applied in scientific research and clinical treatment.<sup>[4–6]</sup> However, many biopharmaceuticals suffer from problems such as inferior biophysical stability and propensity in aggregation or degradation.<sup>[7,8]</sup> Temperature alteration, mechanical force impact, chemical reagent corrosion, and other perturbation environments can cause the degradation of therapeutic proteins, and lead to adverse impact on the efficacy.<sup>[9]</sup> Thus, biopharmaceuticals are usually required to be maintained under tightly regulated conditions (e.g., 4 °C refrigeration). Meanwhile, for preparation, transportation, or storage purpose, a variety of approaches such as isothermal vitrification<sup>[10]</sup> and lyophilization<sup>[11]</sup> are com-

monly required with additives (e.g., glycerin, trehalose, and bull serum albumin (BSA)) to stabilize proteins.<sup>[12]</sup> However, these regulated conditions and complicated processes tremendously raise the cost and introduce extra biosafety risks for the applications of biopharmaceuticals. For example, vitrification and lyophilization of protein with sugars may cause aggregation or unpredictable immunogenicity due to the lack of control of sugar crystallization.<sup>[13]</sup> Although polymers have been proposed as additives to enhance thermal stability of proteins,<sup>[14]</sup> problems such as separation difficulty and possible immunological risks still remain. Therefore, developing facile and efficient strategies to stabilize biopharmaceuticals is urgently demanded.

Emerging as a new class of crystalline solid-state materials,<sup>[15]</sup> metal–organic frameworks (MOFs) feature high porosity, tunable pore size and facily tailored functionality.<sup>[16,17]</sup> These merits make MOFs hold promise for many applications including catalysis,<sup>[18–20]</sup> gas storage,<sup>[21,22]</sup> sensors,<sup>[23,24]</sup> and functional devices.<sup>[25,26]</sup> Although recent studies revealed MOFs' great potential in biomedical applications,<sup>[27–30]</sup> the development of MOFs as biomedical materials is still in its infancy with many challenges to be addressed.<sup>[31,32]</sup> Some primary concerns have been recognized to be the biocompatibilities of MOFs. Traditionally, the encapsulated proteins must

Y. Feng, H. Wang, S. Zhang, Y. Zheng, Prof. Z. Zhang, Prof. Y. Chen  
State Key Laboratory of Medicinal Chemical biology  
Nankai University  
Tianjin 300071, China  
E-mail: chenyaoyao@nankai.edu.cn

Y. Zhao, Dr. J. Gao, P. Zhao, Prof. Z. Zhang, Prof. P. Cheng  
College of Chemistry  
Nankai University  
Tianjin 300071, China

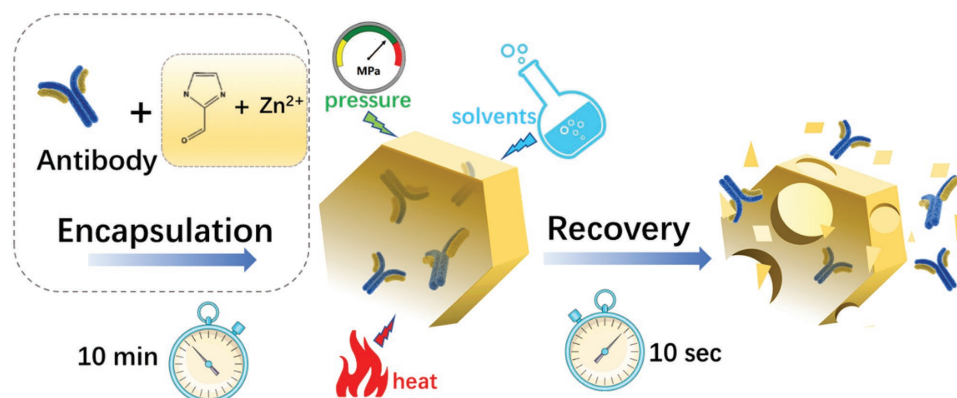
Prof. M. J. Zaworotko  
Department of Chemical Sciences  
Bernal Institute  
University of Limerick  
Limerick V94XT66, Republic of Ireland

Prof. S. Ma  
Department of Chemistry  
University of South Florida  
Tampa, FL 33620, USA  
E-mail: sqma@usf.edu

Prof. Y. Chen  
College of Pharmacy  
Nankai University  
Tianjin 300071, China

 The ORCID identification number(s) for the author(s) of this article can be found under <https://doi.org/10.1002/adma.201805148>.

DOI: 10.1002/adma.201805148



**Scheme 1.** Schematic illustration of in vitro protective coating strategy for antibody preparation and applications.

enter the body accompanied by their carriers due to the great separation difficulty and possible adverse impact on biomolecules' activities during the removal of materials. However, materials may introduce biocompatibility issues and immunological risks. To circumvent those above, herein, we developed a facile strategy as a potential new formulation method for biopharmaceuticals as represented by antibodies. This in vitro protective coating strategy can quickly encapsulate and release antibodies with high efficiency using various MOFs platforms, which can be employed to protect biopharmaceuticals without introducing the additives (MOFs) into body thereby avoiding potential biocompatibility risks (**Scheme 1**). To demonstrate the generality of our strategy, two prototypical zeolite imidazolate frameworks (ZIF-90 and ZIF-8) were used as representative MOFs in this study. ZIF-90 and ZIF-8 both exhibit excellent ability to immobilize a wide range of guest molecules (e.g., nanoparticle, drugs, enzymes, etc.).<sup>[33–37]</sup> Moreover, they can be degraded to release the incorporated guest molecules under mild conditions. These features together with the outstanding biocompatibility (e.g., low cytotoxicity) and exceptional water stability make ZIF-90 and ZIF-8 perfect platforms to accommodate biopharmaceuticals.

Several antibodies were used as the model molecules in this study. Two thoroughly researched antibodies, Human immunoglobulin G (IgG) polyclonal antibody (H-IgG) and Goat anti BSA IgG polyclonal antibody (G-IgG), were selected to represent polyclonal antibodies. H-IgG is a kind of mixture of human antibodies purified from human serum. It was used here to study the influence on antibody's structure during the MOF encapsulation process because it is one of the most abundant antibodies both in blood and body fluids (75%–80% of total serum antibodies). G-IgG from goat serum have active binding to BSA for easy assessment of its activity (e.g., enzyme-linked immunosorbent assay (ELISA) assay) and thus was used to verify MOFs' impact on antibody's activity. In addition, a marketed monoclonal antibody, adalimumab (Ada), was also used in this study to further proof the universality of our strategy. Adalimumab is a tumor necrosis factor (TNF)-inhibiting, anti-inflammatory, biologic medication, which was one of the first approved human monoclonal antibodies for therapeutic applications. This study provides a new MOF-based strategy to stabilize biopharmaceuticals for their facile preparation and storage without introducing biocompatibility

risks, and bridges the gap between the developed MOFs materials and their practical biomedical applications.

MOFs are reported to form porous shells that can encapsulate biomolecules via self-assembly under mild conditions.<sup>[38,39]</sup> We selected ZIF-90 and ZIF-8 as representative materials and first investigated their encapsulation of antibodies (H-IgG and G-IgG). The encapsulation conditions for each antibody were optimized based on a balance of the productivity of antibodies@MOFs and their loading capacities of antibodies. To be specific, the encapsulation of antibodies was first conducted using various antibody concentrations (0.5–1.5 mg mL<sup>-1</sup>), and the productivity, crystallinity, and loading efficiency of the afforded composites were examined. We found that low productivity of antibodies@MOFs was observed when using antibody concentrations of  $\leq 0.5$  mg mL<sup>-1</sup>, and high antibody concentrations ( $\geq 1.5$  mg mL<sup>-1</sup>) lead to low loading capacities. Therefore, to balance productivity and loading capacities, the 1.0 mg mL<sup>-1</sup> of antibody concentration was selected as the encapsulation condition for further investigation. The encapsulation efficiency and loading capacities was determined via a standard Bradford assay method. As shown in **Figure 1** and Table S1 in the Supporting Information), all the tested antibodies@MOFs systems (H-IgG@ZIF-90, H-IgG@ZIF-8, G-IgG@ZIF-90, and G-IgG@ZIF-8) can quickly complete the encapsulation within 10 min with high encapsulation efficiencies (>99%) and high loading capacities (0.53  $\pm$  0.03 g/g for H-IgG@ZIF-90, 0.37  $\pm$  0.01 g/g for H-IgG@ZIF-8, 0.59  $\pm$  0.02 g/g for G-IgG@ZIF-90, 0.42  $\pm$  0.03 g/g for G-IgG@ZIF-8) of antibodies.

We then characterized the formed antibodies@MOFs using various instruments (**Figures 2 and 3** and Figures S1 and S2, Supporting Information). The crystallinity of antibodies@MOFs was assessed by powder X-ray diffraction (PXRD) studies, which revealed that the crystal structure integrities of antibodies@MOFs are consistent with pristine MOFs (Figure 2a,b). Scanning electron microscopy (SEM) images showed all antibodies@ZIF-8 systems emerged the same polyhedral morphology as pristine ZIF-8, whereas, antibodies@ZIF-90 possesses a flat saucer-shaped morphology (Figure 3a,b), which is different from that of pristine ZIF-90. We speculated that the different morphologies could be ascribed to the template effect of biomacromolecules during the formation of ZIF-90 particles. Fourier transform infrared (FT-IR) spectroscopy was used to ascertain if antibodies were

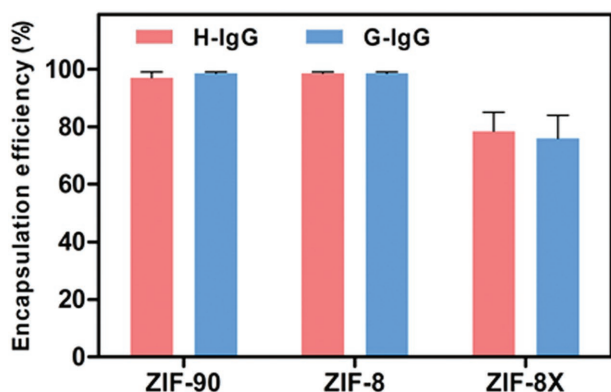


**Figure 1.** The antibodies encapsulation efficiency of antibodies@MOFs. *P*-value for H-IgG and G-IgG encapsulating in the same MOF is 0.665; *P*-value for different MOFs encapsulating the same antibody is  $<5 \times 10^{-7}$ .

indeed encapsulated into MOFs (Figure 2c,d). The spectra of antibodies@MOFs showed stretches at  $1530 \text{ cm}^{-1}$  for antibodies, corresponding to characteristic amide II band (mainly from a combination of  $-\text{NH}$  bending and  $-\text{CN}$  stretching modes). In addition, FT-IR spectra of both H-IgG@MOFs and G-IgG@MOFs showed that the amide vibrational mode for the antibodies shifted toward higher wave numbers compared with pristine MOFs, indicative of the strong interactions between the

antibody and MOFs. The FT-IR results suggested the successful encapsulation of proteins into the pores of MOFs. To further verify the successful encapsulation of antibodies, fluorescein isothiocyanate (FITC)-labeled H-IgG and G-IgG were encapsulated by ZIF-90 and ZIF-8 (Figure S2, Supporting Information). The fluorescence signal of FITC-labeled IgGs uniformly distributed thoroughly in the resultant composite, which is attributed to the encapsulated FITC-labeled IgGs. In contrast, pristine ZIF-8 and ZIF-90 were not emissive (Figure S2, Supporting Information). Besides ZIF-90 and ZIF-8, we also discovered an unknown MOF (ZIF-8X) with cruciate flower-like morphology (particle  $\approx 400 \text{ nm}$ ) formed during the synthesis process of ZIF-8<sup>[40]</sup> (Figure S3, Supporting Information). Based on elemental analysis, the molecular formula of ZIF-8X is determined to be  $[\text{Zn}(\text{2-methylimidazole})_2]_n$  (Table S2, Supporting Information). We found ZIF-8X can also encapsulate antibodies, but with much lower efficiency than ZIF-8 and ZIF-90 (Figure 1a).

To avoid possible biosafety risks from MOFs, it is better to remove MOFs from antibodies@MOFs composite to recover the antibodies before usage. Some MOFs have been reported to degrade after treatment with acid<sup>[39]</sup> or chelating agents.<sup>[41]</sup> Inspired by this, we developed facile strategies to recover the encapsulated antibodies and evaluated the recovery efficiency. We firstly optimized the recovery strategies

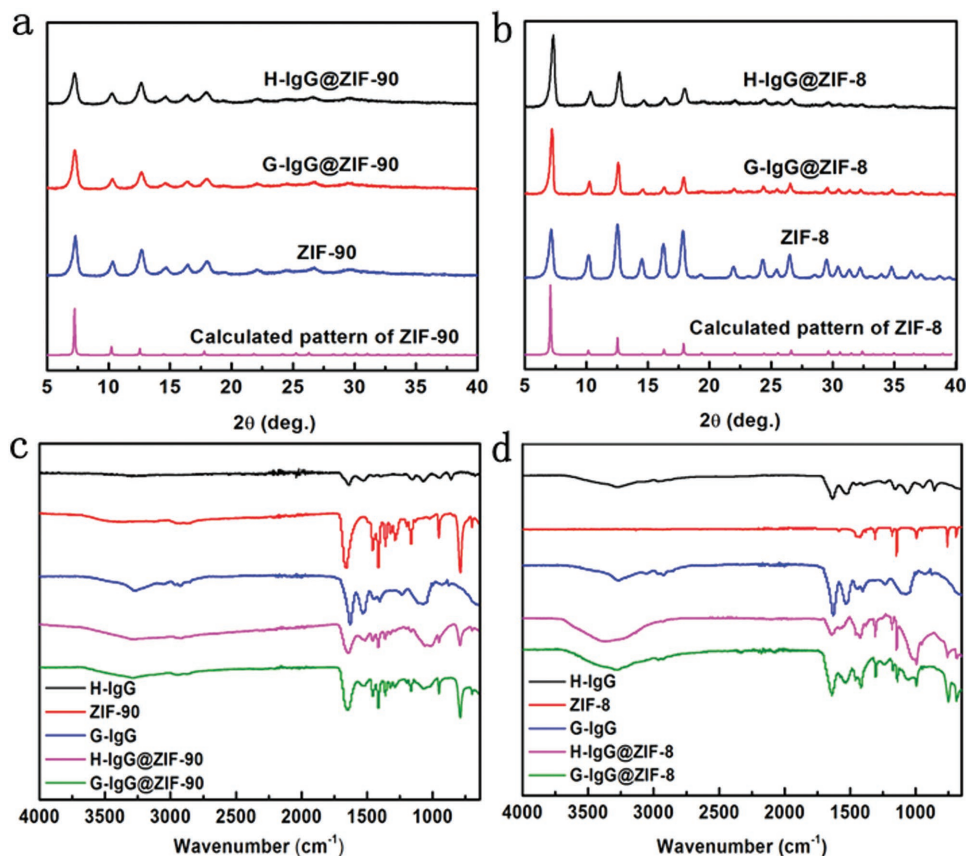


**Figure 2.** a) Experimental PXRD patterns of H-IgG@ZIF-90, G-IgG@ZIF-90, pristine ZIF-90 compared with calculated pattern of ZIF-90. b) Experimental PXRD patterns of H-IgG@ZIF-8, G-IgG@ZIF-8, pristine ZIF-8 compared with calculated pattern of ZIF-8. c) FT-IR spectra of H-IgG, pristine ZIF-90, G-IgG, H-IgG@ZIF-90, and G-IgG@ZIF-90. d) FT-IR spectra of H-IgG, pristine ZIF-8, G-IgG, H-IgG@ZIF-8, and G-IgG@ZIF-8.

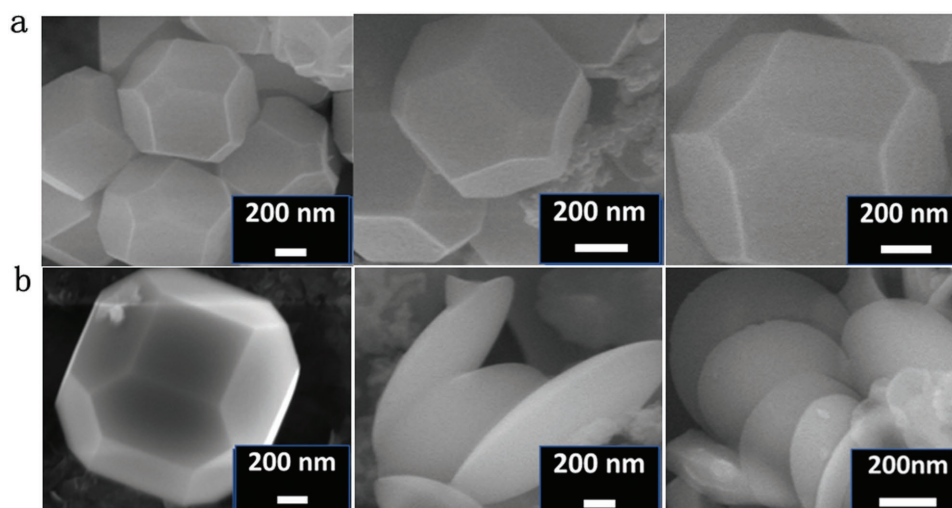


**Figure 3.** a) SEM images of pristine ZIF-8 (left), H-IgG@ZIF-8 (middle), and G-IgG@ZIF-8 (right). b) SEM images of pristine ZIF-90 (left), H-IgG@ZIF-90 (middle), and G-IgG@ZIF-90 (right).

for each antibodies@MOFs system. Taking antibodies@ZIF-90 as an example, we used different releasing agents such as ethylenediaminetetraacetic acid (EDTA), citric acid phosphate buffer with different pH values (e.g., pH 4.5, 5, 6, 7), and evaluated the recovery efficiency, including releasing rates (Table S3, Supporting Information). Finally, we found that antibodies can be efficiently released within 10 s from ZIF-90 in acid phosphate buffer (pH 4.5). Antibodies@ZIF-8 and antibodies@ZIF-8X completed the releasing within 30 min in EDTA (pH 5.0). The released antibodies can be simply separated from MOFs and recovered by ultrafiltration with 100 kDa MWCO (molecular weight cut off) devices, which can harvest pure antibodies due to the great molecular weight differences between IgG ( $\approx 150$  kDa) and the impurities (e.g., digested ligands, metal salts). The recovery efficiency was defined as the ratio of recovered antibodies to the initial encapsulated antibodies. We found all the tested antibodies@MOFs systems demonstrated high recovery efficiencies ( $>85\%$ ), among which H-IgG@ZIF-90, G-IgG@ZIF-90, H-IgG@ZIF-8, and G-IgG@ZIF-8 showed recovery efficiencies of 92%, 88%, 93%, and 95%, respectively (Figure 4a). Thus, nearly all the encapsulated antibodies can be recovered from MOFs under optimized conditions. Notably, antibodies@ZIF-90 and antibodies@ZIF-8

can finish their antibody release within short timeframes ( $\approx 10$  s and  $\approx 30$  min, respectively). More importantly, the ELISA assay results verified that the recovered antibody (e.g., G-IgG) remained the same activity as original antibody (Figure 4b). In order to verify if there were residues from MOFs (e.g., MOFs, metal salts, or ligands residue) remained in the recovered antibodies, we used various techniques including PXRD, energy dispersive X-ray spectroscopy (EDX) and elemental analysis to characterize the recovered antibodies. PXRD pattern of the recovered antibodies showed that there were no peaks assigned to MOFs (Figure S4, Supporting Information), implying the complete removal of MOFs. Additionally, comparison of the EDX results for pristine antibodies and recovered antibodies (Figures S5 and S6, Supporting Information) revealed that no zinc metal residue remained in the recovered antibodies. Moreover, the elemental analysis of antibodies recovered from antibodies@MOFs agreed well with the pristine antibodies (Table S4, Supporting Information), which further proved the elimination of residues from MOFs including the ligands.

We also investigated the influence on antibodies' structural integrities and activities in the encapsulation and recovery process. To check the structural integrity of antibodies reclaimed

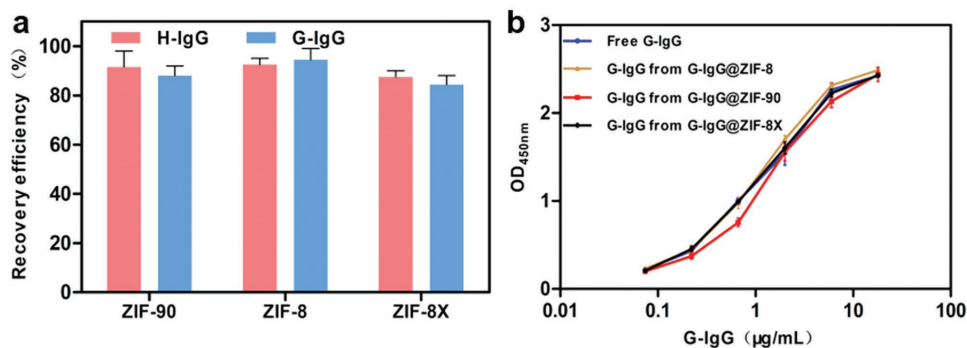


**Figure 4.** a) Antibodies recovery efficiency of antibodies@MOFs. b) Indirect ELISA assay results of free G-IgG and G-IgG released from antibodies@MOFs. The OD<sub>450</sub> data reflects the bioactivity of the tested samples, and the results show the recovered antibodies possess the same signal as the original antibody, indicating retained bioactivities.

from MOFs, we used sodium dodecyl sulfate-polyacrylamide gel electrophoresis (SDS-PAGE) to evaluate the integrity of recovered G-IgG with or without reducing agents. The results of nonreducing experiments confirmed the overall integrity of the recovered G-IgG, and the results with reducing condition further proved the integrity of heavy and light chains in the recovered G-IgG (two main bands at  $\approx 50$  and 25 kDa, Figure S7, Supporting Information) as well as the basic functional unit of G-IgG. Therefore, the SDS-PAGE test indicated that G-IgG recovered from MOFs maintained their structural integrity with no aggregation or cleavage. In addition, the activities of the recovered G-IgG were evaluated by indirect-ELISA, and their binding capacities were compared with that of untreated G-IgG. We observed that the recovered G-IgG possessed same binding capacities as untreated G-IgG in all the tested systems (Figure 4b), suggesting the preserved bioactivities of antibodies during the encapsulation and recovery process. The well retained antibodies' structures and activities, associated with the quick encapsulation and recovery process, are essential for practical applications, which endowed our strategy great potentials for biomedical applications.

In order to study our strategy's protection effect on antibodies, G-IgG@ZIF-90 and G-IgG@ZIF-8 were treated in a series of perturbation environments that would normally lead to antibodies' denaturation or loss of activities, including high temperature, organic solvents, freeze-thawing cycles, and mechanical pressure. After treatment, the protected antibodies were recovered from antibodies@MOFs and compared with the unprotected antibodies that were treated under the same conditions. The binding activity and aggregation rate of the recovered antibodies were evaluated as criterion of stability to assess antibodies' structural integrity and bioactivity after the treatments, which were determined by ELISA and size exclusion chromatography HPLC (SEC-HPLC).

IgGs@MOFs and free IgGs were exposed at 75 °C to test the thermal protection effect of MOFs. The unprotected G-IgG and H-IgG exhibited severe aggregation (88% and 99%) after heating (Figure 5a). In contrast, G-IgG and H-IgG coated by ZIF-90 and ZIF-8 showed much lower aggregation after the same treatment (13–25%). Additionally, ELISA assay showed that G-IgG (H-IgG cannot be effectively tested by ELISA due to its nonspecificity) released from MOFs possessed similar binding abilities as their original antigen of untreated G-IgG (>90%), whereas the unprotected G-IgG almost lost all binding activity (<10% of activity, Figure 4). In addition, the circular dichroism (CD) and FT-IR spectra unveiled a significant change in the secondary structure of unprotected antibody, while ZIF-90 and ZIF-8 protected antibody remained its secondary structure after the heat treatment (Figures S8 and S9, Supporting Information). These results highlighted MOFs' excellent thermal protection for antibodies. Moreover, after treatment with organic solvents (e.g., methanol, acetone) for 1 h (Figure 5a), the unprotected G-IgG and H-IgG also showed severe aggregation (>90%) in the presence of methanol or acetone, while G-IgG and H-IgG protected by MOFs exhibited relatively low aggregation (5–25%). In addition, G-IgG recovered from G-IgG@ZIF-90 and G-IgG@ZIF-8 essentially retained their binding capacity ( $\approx 80\%$  determined by ELISA assay), indicating the enhanced chemical resistance. In contrast, the unprotected free G-IgG almost lost its binding

capacity (<10% of activity) after exposure to organic solvent (Figure 5b). Actually, after both of the heating or organic solvent treatments, the unprotected G-IgG samples experienced such a severe aggregation that a large amount of visible particles were observed (Figure S10, Supporting Information). To evaluate antibodies@MOFs' resistance against perturbation conditions such as freezing-thawing cycles (commonly encountered in practical storage and transportation of biopharmaceuticals), G-IgG@ZIF-90, H-IgG@ZIF-90, G-IgG@ZIF-8, and H-IgG@ZIF-8 were treated under alternate freezing-thawing cycles ( $-80^{\circ}\text{C} \leftrightarrow 37^{\circ}\text{C}$ , 10 cycles). After the treatment, G-IgG and H-IgG protected by ZIF-90 and ZIF-8 exhibited <25% of aggregation (Figure 5a). Meanwhile, bioactivity evaluation revealed that G-IgG can still retain >90% of bioactivity after released from ZIF-90 and ZIF-8 (Figure 5b). In contrast, the free G-IgG and H-IgG exhibited  $\approx 70\%$  and  $\approx 60\%$  aggregation, respectively, and significantly lost the bioactivity. To examine antibodies@MOFs' resistance against mechanical pressure, IgGs@MOFs samples were squeezed under 20 MPa pressure using a tablet machine. After the pressure treatment, G-IgG released from ZIF-90 and ZIF-8 retained the bioactivity of 75% and 95%, respectively (Figure 5b). Meanwhile, both of G-IgG and H-IgG released from ZIF-90 and ZIF-8 exhibited <10% aggregation (Figure 5a). The results illustrated that antibodies@MOFs exhibited good resistance against mechanical pressure. Notably, ZIF-8 performed slightly better protection effect than ZIF-90 (Figure 5), which may be attributed to the higher structural stability of ZIF-8. However, ZIF-90 systems depicted a higher encapsulating and recovery speed ( $\approx 10$  min, 10 s, respectively). Overall, based on our strategies, antibodies@MOFs significantly enhanced antibodies' thermal, chemical, and mechanical resistance against perturbation environments, and thus facilitated the easy-operation of antibodies, which may greatly promote their applications.

With the enhanced resistance against perturbation environments, biopharmaceuticals, such as antibodies may be easily stored, operated, and applied under normal or harsh conditions, thus tremendously broadening their applications and reducing the cost. Therefore, to prove the practical usage of our antibodies@MOFs systems, we challenged those systems for long-term storage under severe temperature variation to evaluate their protection capabilities. G-IgG with or without the protection of MOFs were stored under a temperature cycling test condition ( $50 \leftrightarrow 4^{\circ}\text{C}$ ,  $25^{\circ}\text{C min}^{-1}$  ramp rate) for three weeks. The results show that G-IgG with the protection of MOFs can retain  $\approx 90\%$  of binding capability after the three-week storage, while unprotected antibodies lost nearly all activities (Figure 5c). The results clearly proved the extraordinary stabilities of the protected antibodies under severe temperature variation for long term storage, which provides great potentials in biopharmaceuticals preparation and storage, such as development of new portable delivery or long-term storage systems.

To further demonstrate the universality of our strategy and further prove its practical potential, we also tested a marketed biopharmaceutical, adalimumab (Ada), which is a widely used therapeutic monoclonal antibody. Our results showed that Ada could be successfully encapsulated with > 99% encapsulation efficiency and recovered with high efficiency (>90%) as well (Figure 5d and Figure S11, Supporting Information).

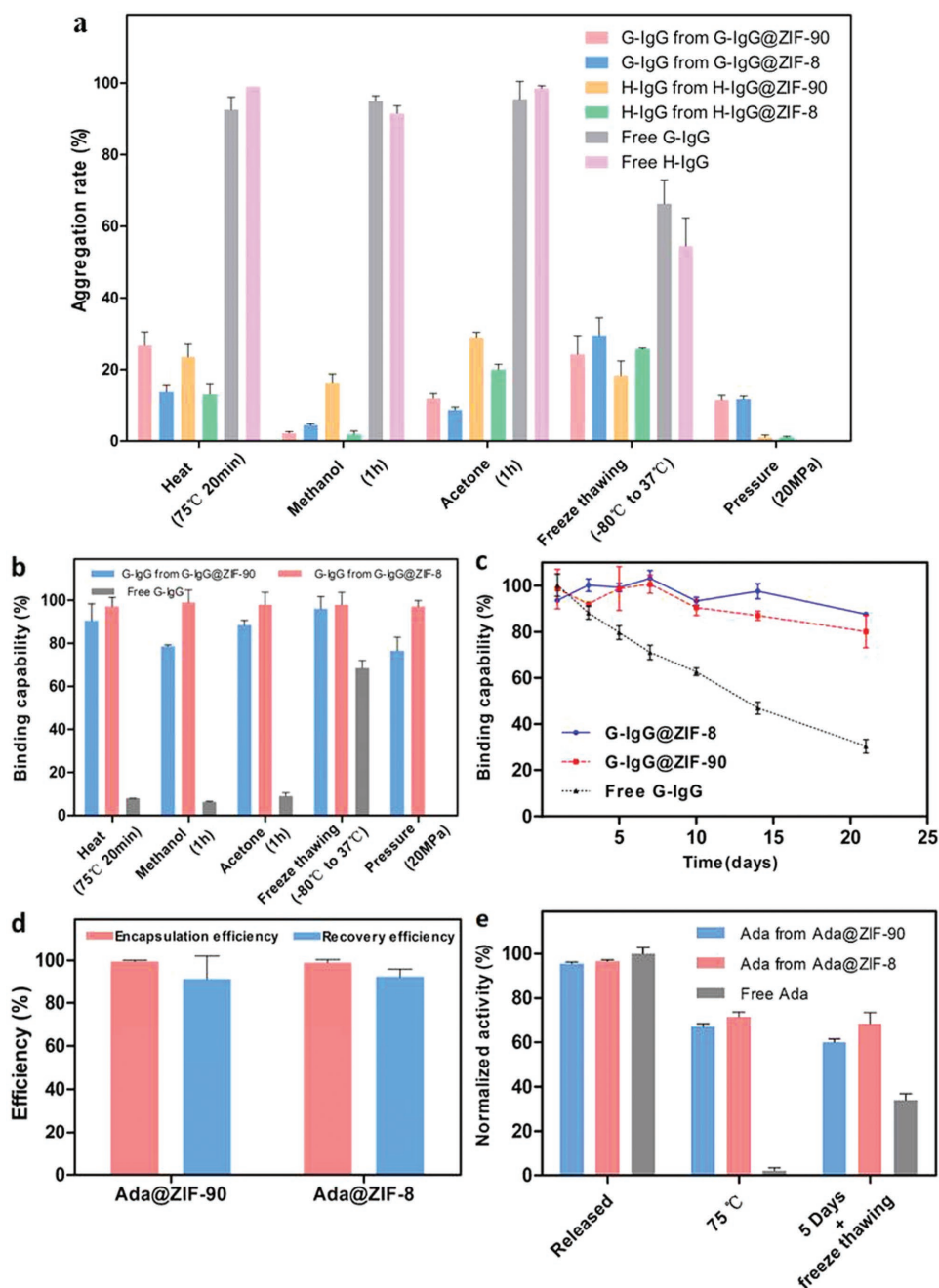


**Figure 5.** a) Aggregation rate of protected IgGs and free IgGs after the treatment with various perturbation conditions. b) Binding capacity of protected G-IgG and free G-IgG after treatment with various perturbation conditions. c) Protective performance of MOFs for G-IgG in the long-term storage test. d) The Ada encapsulation efficiency of Ada@MOFs and Ada recovery efficiency of Ada@MOFs. e) Bioactivity of Ada recovered from Ada@MOFs. Binding capacity of protected Ada and free Ada after treatment with various perturbation conditions: 75 °C heat; 5 days storage under temperature variation (4 ↔ 50 °C) at fast ramp rate (25 °C min<sup>-1</sup>) + 10 freeze-thawing cycles (-80 °C–37 °C).

The indirect ELISA assay revealed that the recovered Ada antibody retained its activity (>90% activity of original antibody). In addition, after treatment with various perturbation conditions (75 °C heat; 5 days storage under temperature variation + 10 freeze thawing cycles), the binding capacity of protected Ada still retained >60%, whereas free Ada dramatically lost its activity after the treatments and exhibited severe aggregation (Figure 5e and Figure S12, Supporting Information). These

results again highlighted the great application potential of our strategy in biopharmaceuticals preparation and storage.

In conclusion, we developed a facile and efficient strategy for antibodies' preparation and storage using MOFs as removable shells with prominent protection effect. Besides the high encapsulation efficiency (>99%), the formed antibodies@MOFs exhibited enhanced resistance against perturbation environments, such as heating, organic solvents, and

mechanical pressure, and can survive for long term storage (>3 weeks) under temperature cycling test condition at fast ramp rate. These extraordinary properties will greatly broaden the operational conditions that can be applied for antibodies, and facilitate the preparation, transportation, and storage of related biopharmaceuticals. More importantly, MOFs can be quickly and simply eliminated without interference on the subsequent usage of antibodies, and meanwhile retain their structures and bioactivities, which can avoid possible biocompatibility risks introduced by MOFs. It is noteworthy that the encapsulation and releasing of antibodies using ZIF-90 were completed within very short timeframes ( $\approx 10$  min, 10 s, respectively). This quick response and the outstanding performance endow MOFs great potentials to serve as a versatile platform for biopharmaceuticals preparation and storage. This facile strategy may bridge the gap between the developed MOFs materials and their practical biomedical applications, and provide guidance for the design of facile and efficient long-term storage or portable delivery systems for therapeutic proteins.

## Supporting Information

Supporting Information is available from the Wiley Online Library or from the author.

## Acknowledgements

The authors acknowledge the Young 1000-Plan program and financial support from the National Natural Science Foundation of China (21601093) and Tianjin Natural Science Foundation of China. The authors thank Prof. H. K. Zhang of State Key Laboratory of Medicinal Chemical biology, Nankai University for the immunological test guidance. The authors thank X. T. Tan of University of Michigan for valuable discussions about immunological test.

## Conflict of Interest

The authors declare no conflict of interest.

## Keywords

antibodies, biopharmaceuticals, encapsulate, metal–organic frameworks, release

Received: August 7, 2018

Revised: October 19, 2018

Published online: November 27, 2018

- [1] S. Lawrence, *Nat. Biotechnol.* **2007**, *25*, 1342.
- [2] B. Leader, Q. J. Baca, D. E. Golan, *Nat. Rev. Drug Discovery* **2008**, *7*, 21.
- [3] M. N. Lobato, T. H. Rabbitts, *Trends Mol. Med.* **2003**, *9*, 390.
- [4] D. A. Martin, D. A. Muth, T. Brown, A. J. Johnson, N. Karabatsos, J. T. Roehrig, *J. Clin. Microbiol.* **2000**, *38*, 1823.
- [5] R. L. Ashley, J. Militoni, F. Lee, A. Nahmias, L. Corey, *J. Clin. Microbiol.* **1988**, *26*, 662.
- [6] R. Scully, J. Chen, A. Plug, Y. Xiao, D. Weaver, J. Feunteun, T. Ashley, D. M. Livingston, *Cell* **1997**, *88*, 265.
- [7] E. Y. Chi, S. Krishnan, T. W. Randolph, J. F. Carpenter, *Pharm. Res.* **2003**, *20*, 1325.
- [8] C. J. Roberts, *Biotechnol. Bioeng.* **2007**, *98*, 927.
- [9] A. Braun, L. Kwee, M. A. Labow, J. Alsenz, *Pharm. Res.* **1997**, *14*, 1472.
- [10] R. Less, K. L. Boylan, A. P. Skubitz, A. Aksan, *Cryobiology* **2013**, *66*, 176.
- [11] I. Bakaltcheva, A. M. O'Sullivan, P. Hmel, H. Ogbu, *Thromb. Res.* **2007**, *120*, 105.
- [12] B. P. Best, *Rejuvenation Res.* **2015**, *18*, 422.
- [13] S. K. Singh, P. Kolhe, A. P. Mehta, S. C. Chico, A. L. Lary, M. Huang, *Pharm. Res.* **2011**, *28*, 873.
- [14] N. Martin, D. Ma, A. Herbet, D. Boquet, F. M. Winnik, C. Tribet, *Biomacromolecules* **2014**, *15*, 2952.
- [15] H. C. Zhou, J. R. Long, O. M. Yaghi, *Chem. Rev.* **2012**, *112*, 673.
- [16] H. Furukawa, K. E. Cordova, M. O'Keeffe, O. M. Yaghi, *Science* **2013**, *341*, 1230444.
- [17] H. C. Zhou, S. Kitagawa, *Chem. Soc. Rev.* **2014**, *43*, 5415.
- [18] A. Corma, H. García, F. X. Llabrés i Xamena, *Chem. Rev.* **2010**, *110*, 4606.
- [19] Z. Niu, W. D. C. B. Gunatilleke, Q. Sun, P. C. Lan, J. Perman, J.-G. Ma, Y. Cheng, B. Aguila, S. Ma, *Chem* **2018**, *4*, 2587.
- [20] Y. B. Huang, J. Liang, X. S. Wang, R. Cao, *Chem. Soc. Rev.* **2017**, *46*, 126.
- [21] H. Li, K. Wang, Y. Sun, C. T. Lollar, J. Li, H.-C. Zhou, *Mater. Today* **2018**, *21*, 108.
- [22] S. Ma, H.-C. Zhou, *Chem. Commun.* **2010**, *46*, 44.
- [23] F.-Y. Yi, D. Chen, M.-K. Wu, L. Han, H.-L. Jiang, *ChemPlusChem* **2016**, *81*, 675.
- [24] L. E. Kreno, K. Leong, O. K. Farha, M. Allendorf, R. P. Van Duyne, J. T. Hupp, *Chem. Rev.* **2012**, *112*, 1105.
- [25] I. Stassen, N. Burtch, A. Talin, P. Falcaro, M. Allendorf, R. Ameloot, *Chem. Soc. Rev.* **2017**, *46*, 3185.
- [26] P. Falcaro, R. Ricco, C. M. Doherty, K. Liang, A. J. Hill, M. J. Styles, *Chem. Soc. Rev.* **2014**, *43*, 5513.
- [27] T. Simon-Yarza, M. Giménez-Marqués, R. Mrimi, A. Mielcarek, R. Gref, P. Horcajada, C. Serre, P. Couvreur, *Angew. Chem., Int. Ed.* **2017**, *56*, 15565.
- [28] Y. Chen, V. Lykourinou, C. Vetromile, T. Hoang, J. Ming, R. W. Larsen, S. Ma, *J. Am. Chem. Soc.* **2012**, *134*, 13188.
- [29] X. Pan, L. Bai, H. Wang, Q. Wu, H. Wang, S. Liu, B. Xu, X. Shi, H. Liu, *Adv. Mater.* **2018**, *30*, 1800180.
- [30] J. Zhuang, C. H. Kuo, L. Y. Chou, D. Y. Liu, E. Weerapana, C. K. Tsung, *ACS Nano* **2014**, *8*, 2812.
- [31] M. X. Wu, Y. W. Yang, *Adv. Mater.* **2017**, *29*, 1606134.
- [32] C. Wang, J. Gao, H. Tan, *ACS Appl. Mater. Interfaces* **2018**, *10*, 25113.
- [33] W. Liang, R. Ricco, N. K. Maddigan, R. P. Dickinson, H. Xu, Q. Li, C. J. Sumbly, S. G. Bell, P. Falcaro, C. J. Doonan, *Chem. Mater.* **2018**, *30*, 1069.
- [34] Q. Wang, X. Zhang, L. Huang, Z. Zhang, S. Dong, *Angew. Chem., Int. Ed.* **2017**, *129*, 16298.
- [35] N. Liédana, A. Galve, C. Rubio, C. Téllez, J. Coronas, *ACS Appl. Mater. Interfaces* **2012**, *4*, 5016.
- [36] X. Qiao, B. Su, C. Liu, Q. Song, D. Luo, G. Mo, T. Wang, *Adv. Mater.* **2018**, *30*, 1702275.
- [37] F. M. Zhang, H. Dong, X. Zhang, X. J. Sun, M. Liu, D. D. Yang, X. Liu, J. Z. Wei, *ACS Appl. Mater. Interfaces* **2017**, *9*, 27332.
- [38] P. Horcajada, R. Gref, T. Baati, P. K. Allan, G. Maurin, P. Couvreur, G. Ferey, R. E. Morris, C. Serre, *Chem. Rev.* **2012**, *112*, 1232.
- [39] K. Liang, R. Ricco, C. M. Doherty, M. J. Styles, S. Bell, N. Kirby, S. H. Mudie, D. Haylock, A. J. Hill, C. J. Doonan, P. Falcaro, *Nat. Commun.* **2015**, *6*, 7240.
- [40] J. Cui, Y. Feng, L. Tao, Z. Tan, Z. Cheng, S. Jia, *ACS Appl. Mater. Interfaces* **2017**, *9*, 10587.
- [41] F. S. Liao, W. S. Lo, Y. S. Hsu, C. C. Wu, S. C. Wang, F. K. Shieh, J. V. Morabito, L. Y. Chou, K. C. W. Wu, C. K. Tsung, *J. Am. Chem. Soc.* **2017**, *139*, 6530.